

## Integrate and fire infrared detectors

D. D. Coon and A. G. U. Perera

Citation: *Appl. Phys. Lett.* **51**, 1711 (1987); doi: 10.1063/1.98552

View online: <http://dx.doi.org/10.1063/1.98552>

View Table of Contents: <http://apl.aip.org/resource/1/APPLAB/v51/i21>

Published by the [American Institute of Physics](#).

---

### Related Articles

Exclusion, extraction, and junction placement effects in the complementary barrier infrared detector  
*Appl. Phys. Lett.* **102**, 121109 (2013)

Capacitive infrared photodetector for room temperature operation  
*Appl. Phys. Lett.* **102**, 103108 (2013)

UV-visible detector and LED based n-ZnO/p-Si heterojunction formed by electrodeposition  
*AIP Advances* **3**, 032125 (2013)

Study of sensitization process on mid-infrared uncooled PbSe photoconductive detectors leads to high detectivity  
*J. Appl. Phys.* **113**, 103102 (2013)

Plasmonic enhancement of photocurrent in carbon nanotube by Au nanoparticles  
*Appl. Phys. Lett.* **102**, 103102 (2013)

---

### Additional information on *Appl. Phys. Lett.*

Journal Homepage: <http://apl.aip.org/>

Journal Information: [http://apl.aip.org/about/about\\_the\\_journal](http://apl.aip.org/about/about_the_journal)

Top downloads: [http://apl.aip.org/features/most\\_downloaded](http://apl.aip.org/features/most_downloaded)

Information for Authors: <http://apl.aip.org/authors>

## ADVERTISEMENT

**AIP** | Applied Physics  
Letters

**SURFACES AND INTERFACES**  
Focusing on physical, chemical, biological, structural, optical, magnetic and electrical properties of surfaces and interfaces, and more...

**ENERGY CONVERSION AND STORAGE**  
Focusing on all aspects of static and dynamic energy conversion, energy storage, photovoltaics, solar fuels, batteries, capacitors, thermoelectrics, and more...

**EXPLORE WHAT'S NEW IN APL**

**SUBMIT YOUR PAPER NOW!**

# Integrate-and-fire infrared detectors

D. D. Coon and A. G. U. Perera

Applied Technology Laboratory, Department of Physics, University of Pittsburgh, Pittsburgh, Pennsylvania 15260

(Received 8 May 1987; accepted for publication 21 September 1987)

The effect of infrared radiation on spontaneous pulsing of forward biased silicon  $p^+ - n - n^+$  diodes (injection mode devices) at 4.2 K is studied as a means of detecting infrared radiation in the wavelength range of 20–32  $\mu\text{m}$ . A model based on space-charge buildup of phosphorus donors in the  $i$  region is developed to explain the integration and the sudden firing as well as the dependence of firing frequency on infrared flux. Experimentally, a dynamic range of about a million and responsivities of  $9 \times 10^9$  Hz/W (9.6 A/W) have been found in nonoptimized detectors. Theory indicates the possibility of even larger dynamic ranges. Dark pulse rates as low as  $10^{-5}$  Hz have been observed.

Spontaneous pulsing of forward biased silicon  $p^+ - n - n^+$  ( $p-i-n$ ) diodes, at 4.2 K called injection mode devices (IMD's), has previously been studied.<sup>1-5</sup> However, no quantitative model of the firing mechanism has been proposed until recently.<sup>5</sup> This recent modeling of the spontaneous pulsing mechanism of IMD's dealt with the applied bias voltage and the IMD parameters but not with incident infrared (IR) flux. Here, we expand the modeling to include the effect of the incident infrared flux. Our goal is to produce an analytically solvable model which indicates how the relevant device physics and device parameters influence the device operation and performance.

Typically, the output pulses of the IMD's are approximately uniform in height so that infrared intensity information is contained in the temporal pattern or rate of pulsing. Thus, variations in IR intensity are coded by frequency modulation (FM) rather than by amplitude modulation as in the case of conventional detectors. We have found that IMD's possess larger dynamic ranges. In addition, the output pulses are large (3–20 V typical) so that no preamplifiers are required. The electronic simplicity of IMD's suggests utility in connection with large focal plane arrays.

Low temperatures permit  $i$ -region impurities, in this case phosphorus with 45 meV ionization energy, to act as traps with long lifetimes. Impact ionization and IR photoionization of these  $i$ -region impurities result in an increasing space charge (see Fig. 1). This buildup will trigger injection, i.e., the firing of the IMD. The  $R_L C_L$  load in Fig. 1 cuts off the injection current shortly after it is initiated so that the output consists of injection current pulses. If the injected current neutralizes all of the space charge in the  $i$  region, initial conditions will be the same at the start of each cycle and the injection pulses should then occur periodically. However, depending on the device and circuit parameters, injection pulses may neutralize only a portion of the  $i$ -region space charge. This can give rise to different initial conditions and temporal patterns in the output pulse train, while the overall rate of pulsing is still controlled by the incident IR intensity for a given bias voltage. We have found it useful to adjust the bias voltage or other circuit parameters so that the temporal pulsing pattern is simple and periodic.<sup>5</sup> This is associated with mode locking, a topic of current interest in connection with nonlinear systems.<sup>5-8</sup> We have done a de-

tailed experimental study of mode locking which is the subject of another paper.<sup>9</sup>

The space-charge buildup is described by

$$\frac{d\rho}{dt} = \frac{e\sigma_p n I}{h\nu} + n\sigma_i j, \quad (1)$$

where  $\sigma_i$  is the impact ionization cross section,<sup>10,11</sup>  $\sigma_p$  is the photoionization cross section,<sup>12</sup> and  $n$  is the concentration of un-ionized traps.  $I$  is the IR flux on the diode,  $h\nu$  is the energy of the IR photon, and  $\rho$  is the space-charge density. We assume that the space charge is uniform over the diode thickness. The first term incorporates IR photoionization and the second term incorporates impact ionization. From Gauss's law and integration by parts the field at the  $n-i$  interface is found to be

$$F = \frac{1}{D} (V - V_0) + \frac{1}{D\epsilon} \int_0^D x\rho(x)dx, \quad (2)$$

where  $V$  is the voltage across the diode,  $D$  is the  $i$ -region thickness, and  $V_0$  accounts for the Fermi level difference between the  $p$  and  $n$  impurity bands.

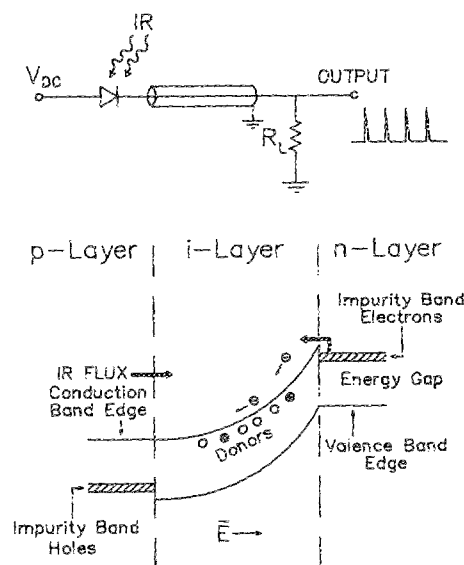


FIG. 1. (a) Circuit diagram showing the experimental setup and the output pulses. The load impedance consists of  $R_L = 50$  K and a cable capacitance  $C_L = 200$  pF. (b) Band diagram for the forward biased  $p-i-n$  diode. Impact ionization causes the  $i$ -region space charge and band bending.

The Richardson–Dushman equation for the injection current density<sup>13–15</sup> becomes

$$j = A * T^2 e^{-(\Delta - edF)/kT}, \quad (3)$$

where  $F$  is the field at the  $n$ - $i$  interface and  $\Delta$  is the energy difference between the conduction-band edge and the  $n$ -region Fermi level.<sup>13</sup> This is analogous to the work function of a metal.  $d$  is the thickness of the transition region<sup>13</sup> associated with the doping profile. The barrier lowering effect, caused by the applied field, is taken into account by the term  $edF$ . This explains the bias voltage dependence of the pulse rate. Combining the above equations, we get

$$j(t) = \frac{bc}{n\sigma_i \{ (c + be^{-ap_0}) e^{-abt} - c \}}, \quad (4)$$

where  $c = n\sigma_i A * T^2 \exp[-\Delta + ed(V - V_0)/D]/kT$ ,  $b = \sigma_p nle/hv$ , and  $a = edD/2\epsilon kT$ . This result reduces to our earlier result<sup>5</sup> when there is no incident infrared flux. Pulses correspond to the singularity in the denominator.

From the above equation, we see that the firing occurs when  $[c + b \exp(-ap_0)] \exp(-abt) = c$  which gives

$$f = f_{\text{dark}} \frac{I/I_0}{\ln(1 + I/I_0)}, \quad (5)$$

where

$$f_{\text{dark}} = \frac{edDc}{2\epsilon kT} e^{ap_0} \quad (6)$$

and

$$\frac{1}{I_0} = \frac{e\sigma_p \exp(-ap_0) \exp(\Delta/kT)}{hv\sigma_i A * T^2 \exp[ed(V - V_0)/DkT]}$$

or

$$\frac{1}{I_0} = \frac{2\epsilon kT n\sigma_p \exp(-ap_0)}{f_{\text{dark}} dDhv}$$

Equation (5) gives rise to Figs. 2 and 3.  $I/I_0 = 0$  gives the dark pulse rate which was calculated to be  $2.2 \times 10^{-5}$  Hz for a particular diode with  $i$ -region thickness,  $D = 100 \mu\text{m}$ , an area  $A = 10^{-2} \text{ cm}^2$  and an impurity concentration of  $3 \times 10^{13} \text{ cm}^{-3}$  for a bias voltage ( $V$ ) of 3.5 V and a value<sup>13</sup> of  $d/D = 6 \times 10^{-3}$  and assuming complete neutralization (i.e.,  $\rho_0 = 0$ ). (This very low frequency seems reasonable because for that particular diode, without any incident IR radiation,

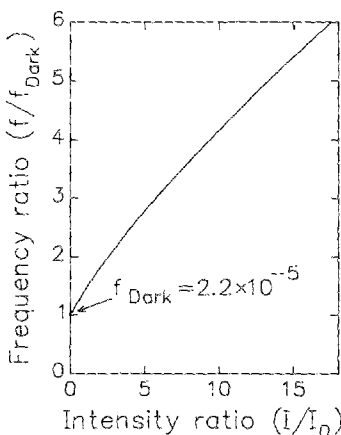


FIG. 2. Pulse rate vs incident IR flux for very low incident flux.

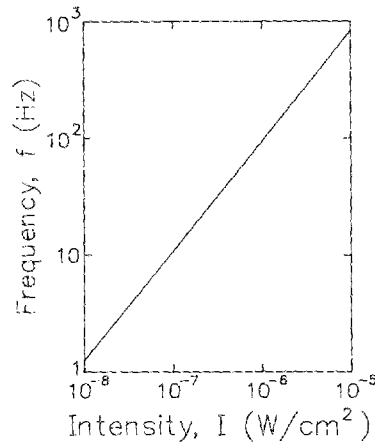


FIG. 3. Pulse rate vs incident IR flux in the range of experimental interest.

24 h elapsed with no pulse observed.) The observed output pulse rate for an input intensity of  $10^{-9} \text{ W/cm}^2$  is about 0.15 per second. This rate is interesting for integrating IR detector applications.<sup>16,17</sup> There is of course the possibility of changing the low-intensity firing rate by changing the device parameters to suit practical applications. Figure 3 corresponds to a higher infrared intensity region. For  $I/I_0 = 1.6 \times 10^8$ ,  $I_0$  being  $1.27 \times 10^{-14} \text{ W/cm}^2$ , the theoretical curve corresponds to a frequency of 180 Hz while experiment yields a value of 185 Hz. Considering the simple picture associated with this model (e.g., uniform space-charge density) and that the exponential ranges over 12 decades, the agreement is remarkably good. Experimentally, we have seen the dynamic range to be a million. This was achieved with a range of IR source temperatures and field-of-view limiting apertures. Although the theoretical dynamic range is much higher than one million, this range well beyond  $10^6$  is not fully useful in practice, as part of the range is associated with extremely low dark pulse rates. Low dark pulse rates are desirable, but interpulse time intervals which are greater than IR exposure times are not useful for intensity measurements. Current responsivity ( $R$ ) is given by  $q df/dI$ , where  $q$  is the charge per pulse,  $df$  is the change of frequency of the output pulse rate, and  $dI$  is the change of incident IR flux. For high intensities (i.e.,  $I/I_0 \gg 1$ ) the frequency responsivity  $df/dI$  becomes

$$\frac{df}{dI} = \frac{f_{\text{dark}}}{I_0} \frac{\ln(I/I_0) - 1}{[\ln(I/I_0)]^2}$$

This is related to the current responsivity which, for a nonoptimized device, has been observed to be 9.6 A/W or  $9 \times 10^9 \text{ Hz/W}$  with power incident on the diode being  $2 \times 10^{-2} \text{ W/cm}^2$ .

Noise equivalent power is given by  $A(dI/df)(\delta f)$ , where  $A$  is the area of the diode,  $dI/df$  is the frequency responsivity, and  $\delta f$  is the variation of the dark pulse rate. Specific detectivity ( $D^*$ ) can be obtained from noise equivalent power. For example, for a particular (nonoptimized) detector at 16.5 V bias, we observe a dark pulse rate of 0.14 Hz over a 50-s interval with a  $\delta f = 0.005 \text{ Hz}$  which corresponds to  $D^* = 3 \times 10^{12} \text{ cm Hz}^{1/2} \text{ W}^{-1}$  for the 27- $\mu\text{m}$  region, where the detector has its highest sensitivity. For comparison with other published results, we note that the

blocked-impurity-band (BIB) detectors<sup>18</sup> of Rockwell have a  $D^*$  of about  $6 \times 10^{12} \text{ cm Hz}^{1/2} \text{ W}^{-1}$  and a responsivity of 6.5 A/W. Our experimental value for  $D^*$  seems remarkable considering the fact that the detector has not been optimized. (As mentioned above the goal of the present work was to develop a model for the devices under study.)

The operation of this integrate-and-fire detector resembles a relaxation oscillator whose output frequency is modulated by infrared radiation. Infrared intensity-to-frequency conversion without *any amplifiers* is a remarkable feature of this IMD. Measuring an interpulse time interval or frequency is much easier than measuring small variations of a very small current as must be done with conventional IR detectors. Very low power consumption and the high amplitude pulse output (3.5 V in the present work) which can be used to fire a light-emitting diode are additional advantages of this mode of IR detection. The large amplitude pulses do not create a problem for heat dissipation for two reasons. One is that the output is not continuous but consists of fast pulses with a dissipation energy of about 0.6 nJ per pulse. In addition the low operating temperature is associated with low leakage current and a quiescent power drain of about 1 nW/cm<sup>2</sup>. Cryogenic temperatures may not be desirable for some applications but for an IR imaging system operation in a cryogenic environment is an advantage. High responsivities, low dark currents, a wide range of response, 20–32  $\mu\text{m}$ , and other factors mentioned above tend to make this detector especially interesting.

This work was supported in part by the U.S. National Science Foundation under Grant No. ECS-8603075.

- <sup>1</sup>D. D. Coon and S. D. Gunapala, *J. Appl. Phys.* **57**, 5525 (1985).
- <sup>2</sup>D. D. Coon and A. G. U. Perera, *Solid-State Electron.* **29**, 929 (1986).
- <sup>3</sup>L. H. De Vaux, U. S. Patent No. 3 466 448 (1969).
- <sup>4</sup>D. D. Coon and A. G. U. Perera, *Int. J. Electron.* **63**, 61 (1987).
- <sup>5</sup>D. D. Coon, S. N. Ma, and A. G. U. Perera, *Phys. Rev. Lett.* **58**, 1139 (1987).
- <sup>6</sup>P. Bak, T. Bohr, and M. H. Jensen, *Phys. Scr.* **T9**, 50 (1985).
- <sup>7</sup>P. Cvitanovic, M. H. Jensen, L. P. Kadanoff, and I. Procaccia, *Phys. Rev. Lett.* **55**, 343 (1985).
- <sup>8</sup>L. Glass and R. Perez, *Phys. Rev. Lett.* **48**, 1772 (1982).
- <sup>9</sup>D. D. Coon and A. G. U. Perera, *Appl. Phys. Lett.* **51**, 1086 (1987).
- <sup>10</sup>N. F. Mott, *Metal-Insulator Transitions* (Barnes and Noble, New York, 1974).
- <sup>11</sup>A. G. Milnes, *Deep Impurities in Semiconductors* (Wiley, New York, 1973), p. 379.
- <sup>12</sup>D. D. Coon and R. F. G. Karunasiri, *Solid-State Electron.* **26**, 1151 (1983).
- <sup>13</sup>Y. N. Yang, D. D. Coon, and P. F. Shepard, *Appl. Phys. Lett.* **45**, 752 (1984).
- <sup>14</sup>S. M. Sze, *Physics of Semiconductor Devices* (Wiley, New York, 1969).
- <sup>15</sup>A. Sommerfeld and H. Bethe, *Handb. Phys.* **24**, 333 (1933).
- <sup>16</sup>M. Harwit, J. R. Houck, B. T. Soifer, and G. G. C. Palumbo, *Astrophys. J.* **315**, 28 (1987).
- <sup>17</sup>B. T. Soifer, D. B. Sanders, B. F. Madore, G. Neugebauer, G. E. Danielson, J. H. Elias, C. J. Persson, and W. L. Rice, *Astrophys. J.* **320**, 238 (1987).
- <sup>18</sup>S. B. Stetson, D. B. Reynolds, M. G. Stapelbroek, and R. L. Stermer, *Infrared Detectors, Sensors and Focal Plane Arrays*, *SPIE* **686**, 48 (1986).